CATASTROPHIC IMPACTS IN THE GRAVITY REGIME; S. G. Love and T. J. Ahrens, Seismological Laboratory 252-21, California Institute of Technology, Pasadena, CA 91125, USA.

The collisional evolution of the asteroids is often modelled by analogy with small-scale, strength dominated laboratory impact experiments [1, 2]. Recent calculations [3], however, suggest that gravity dominates over strength in determining impact behavior for silicate objects larger than ~6 km diameter. Thus, results from strength dominated impacts may not apply to most numbered asteroids or to most meteorite parent bodies. To investigate catastrophic impacts (i.e., those that erode ~50% of the target's mass) on gravity dominated objects, we wrote a three-dimensional Smoothed Particle Hydrodynamics (SPH) computer code that includes a rigorous treatment of gravity. We modelled the impacts of variously sized silicate projectiles onto silicate targets 10 to 1000 km in diameter at impact speeds of 3, 5, or 7 km/s and angles of 15, 45, or 75°. The impact energy is increasingly partitioned into projectile and target kinetic energy at higher impact speeds and larger projectile:target size ratios. Particle velocity distributions are complex in shape and evolve continuously throughout each simulation. The amount of material permanently ejected from the target is roughly proportional to the projectile mass when the speed, angle, and target size are held constant. The catastrophic threshold (Q*) for 50% target mass removal occurs at projectile kinetic energy per unit target mass (specific energy) equal to $8{\cdot}10^3$, $3{\cdot}10^4$, $8{\cdot}10^4$, $3{\cdot}10^5$, and $1.5{\cdot}10^6$ J/kg for target diameters of 10, 31.6, 100, 316, and 1000 km respectively. Projectile material was not retained on targets smaller than 1000 km diameter. The collisions modeled here may launch ejecta into closed satellite orbits. Material strongly heated in our simulations usually escapes; the retained heat produces volume averaged impact heating of <10° C per event for asteroids ≤316 km diameter .

THE MODEL The SPH algorithm [4] models a continuous medium using discrete particles whose physical properties are mathematically "smoothed" out into the neighboring volume. The particle-based SPH method is good for simulating hypervelocity impacts because it remains accurate even when the collision partners suffer extreme geometrical distortion. Our code employs a variable time step and a spherical Gaussian kernel function with a smoothing length (h) equal to the initial cubic lattice separation of the particles. The kernel is truncated at $3h$. The projectile and target materials are represented by the Tillotson [5, 6] equation of state for granite, with a density of 2680 kg/m^3. Targets are represented by 1791 particles; projectiles by 1 to 179 elements of the same size and mass as the target particles. The projectile and target sizes, impact speeds, and impact angles used in the simulations are summarized in Table 1. Most trials employ the likeliest impact angle, 45°. The gravitational force and potential are calculated for each particle using the masses and positions of all other particles in the simulation. We model the hydrodynamic phase of each impact, which includes contact, compression, and propagation of the impact shock wave to the target antipode on a time scale of seconds to minutes. During this time, energy partitioning and evolution of the particle velocity distribution stabilize. Later evolution of the system is primarily ballistic and is treated analytically.

ENERGY PARTITIONING Initial conversion of the projectile's kinetic energy to heat and motion of projectile and target material equilibrates on a timescale of ~4× the projectile diameter divided by the impact speed. The final energy partitioning results are summarized in Table 1. Energy partitioning depends strongly on the impact angle and to a lesser degree on the impact speed. Projectile and target kinetic energies are favored at larger impact speeds and projectile:target diameter ratios. Energy partitioning is relatively independent of the absolute size scale of the event.

VELOCITY DISTRIBUTION The fate of asteroid collision debris in the presence of significant self gravity hinges on its velocity. Particle velocity distributions change constantly in these simulations, evolving rapidly in the hydrodynamic phase and more slowly later as random motions in the target dampen and ballistic ejecta is retarded by gravity. Post hydrodynamic phase velocity distributions (using a 0.2 decade bin width) for all 45°, 5 km/s impacts are shown in Fig. 1. Overlapping curves represent the same projectile:target diameter ratio (Dp/Dt) at different absolute size scales. Single-value or power-law [2] approximations inadequately represent these velocity distributions; a Gaussian in log(velocity) might be more appropriate. A small number of fast particles carry most of the final kinetic energy.

ESCAPING EJECTA Because of the target's distorted geometry during ejecta launch and because some material destined for escape may be launched from deep within the growing crater, comparing particle velocities with the target's surface escape velocity is a poor criterion for escape. Instead, we compare each particle's kinetic energy (K) in the center of mass frame with the gravitational energy (W) that binds it to all other mass in the system. Elements with K≥W escape. Using this criterion, we find that the projectile particles usually escape, except in the case of the 1000 km target where ~3% of the projectile was retained. We also calculate the fraction of the target's mass that is ejected in each impact; results are shown in Table 1. Impact mass erosion is less efficient at shallower impact

angles. At constant target diameter, impact speed, and impact angle, the escaping target mass fraction is roughly proportional to the projectile mass, allowing a simple linear interpolation to estimate Q* [7]. Our values for Q* are much higher than those deduced for the Eos, Themis, and Koronis asteroid family parent bodies [8] and predicted on the basis of laboratory experiments on pressurized targets [3], and are also higher than the targets' intrinsic gravitational binding energy per unit mass, 3GM/(5R), where M is mass, R is radius, and G is the gravitational constant [9]. The latter scales as R^2, while our values scale as $R^{1.13\pm0.01}$; Holsapple [3] predicts $R^{1.67}$ and Davis et al. [10] find $R^{1.5}$. We note that particles with $W>K\geq0.5\cdot W$ are launched onto suborbital trajectories and can reaccrete anywhere on the final rubble pile [11]. Because some ejecta is launched before the target's center of mass begins to move, celestial mechanics permits some of these particles' orbits to close without contacting the surface and raises the possibility of launching asteroid satellites.

IMPACT HEATING Large impacts have been postulated as a heat source for thermal metamorphism within meteorite parent bodies [12]. We can gauge the efficiency of global heating of asteroids in single impacts by finding the internal energy contained in particles that remain bound to the final rubble pile. In spite of the large catastrophic thresholds and substantial fraction of energy partitioned into target heating, we find that most of the strongly heated particles are also strongly accelerated and thus escape. Comparing the retained internal energy to the final target mass yields results as shown in Table 1. Given the ~1300 J/kg-K heat capacity of typical silicates [13], we find that volume averaged target heating in single impacts exceeds 10° C only for targets >316 km diameter.

TABLE 1. IMPACT SIMULATION INITIAL CONDITIONS AND SUMMARY OF RESULTS.

Target Diam. km	Proj. Diam. km	Impact Speed km/s	Impact Angle	Specific Energy J/kg	Final/Initial Target Mass	Proj. I. E. %	Proj. K. E. %	Target I. E. %	Target K. E. %	Retained Target I. E. J/kg (final)
1000	464	5	45°	1 226 000	0.575	10	42	15	33	63 700
316	52.1	5	45°	56 600	0.940	24	17	38	21	2950
316	62.6	5	45°	99 100	0.883	19	19	35	27	3720
316	78.0	3	45°	68 800	0.889	20	27	30	24	2750
316	78.0	5	15°	191 000	0.507	18	6	38	38	6310
316	78.0	5	45°	191 000	0.719	17	28	29	26	4260
316	78.0	5	75°	191 000	0.890	11	63	16	9	3090
316	78.0	7	45°	374 000	0.455	13	30	25	31	7430
316	78.0	7	75°	374 000	0.741	9	65	14	12	4190
316	100.	5	45°	403 000	0.343	15	31	23	32	8340
100.	8.23	5	45°	7 080	0.982	33	14	46	8	355
100.	15.8	5	45°	49 500	0.691	24	18	38	20	450.
100.	19.8	5	45°	99 000	0.382	19	19	35	27	733
31.6	2.60	5	45°	7 200	0.875	33	14	46	8	40.7
31.6	4.99	5	45°	50 400	0.125	24	18	38	20	175
10.0	0.823	5	45°	7 070	0.539	33	14	46	8	7.13

FIG. 1. PARTICLE VELOCITY DISTRIBUTIONS

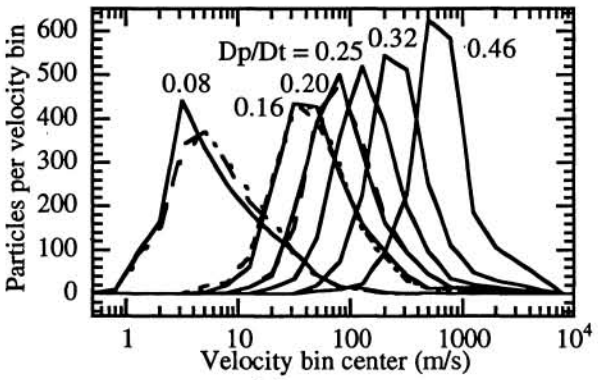

REFERENCES [1] Fujiwara A. et al. (1989) In *Asteroids II* (R. P. Binzel, T. Gehrels, and M. S. Matthews, eds.), 240. [2] Davis D. R. et al. (1985) *Icarus* **62**, 30. [3] Holsapple K. (1994) *Planet. Space Sci.* **42**, 1067. [4] Monaghan J. J. (1992) *Ann. Rev. Astr. Ap.* **30**, 543. [5] Tillotson J. H. (1962) General Atomic Report GA-3216. [6] Melosh J. H. (1989) *Impact Cratering: A Geologic Process*. [7] Ahrens T. J. and Love S. G. (1996) This volume. [8] Fujiwara A. (1982) *Icarus* **52**, 434. [9] Binney J. and Tremaine S. (1987) *Galactic Dynamics*. [10] Davis et al. (1995) LPS XXVI, 319. [11] Benedix G. K. et al. (1996) This volume. [12] Rubin A. E. (1995) *Icarus* **113**, 156. [13] Grieve R. A. F. and Cintala M. J. (1992) *Meteoritics* **27**, 526.